Applied Water Science (2022) 12:148
https://doi.org/10.1007/s13201-022-01674-8

ORIGINAL ARTICLE

Flood hazard assessment and mapping using GIS integrated with multi-criteria decision analysis in upper Awash River basin, Ethiopia

Yonas Gebresilasie Hagos[1,2] · Tesfa Gebrie Andualem[2,3] · Mesenbet Yibeltal[4,5] · Mequanent Abathun Mengie[1]

Received: 6 December 2021 / Accepted: 5 April 2022 / Published online: 6 May 2022

Abstract

Floods have destroyed people's lives as well as social and environmental assets. Flooding is becoming more severe and frequent as a result of climate change and an increase in human-induced land-use changes, which puts pressure on river channels and causes changes in river morphology. The study was aimed to assess flood danger and map inundation areas in Ethiopia's Teji watershed, which is prone to flooding. The basic flood-producing factors in this study were derived from soil, slope, elevation, drainage-density and land use land cover data. The opinions of public institutions and expert decisions were gathered to determine the weight of the factors in the analytic hierarchy process. The collected data were processed using the ArcGIS environment and the analytic hierarchy method to produce a flood danger map. According to the findings of this study, approximately 43.28 and 13.09% of the area were vulnerable to high and very high flood risk zones, respectively. As a result, flood prediction, early warning and management practices could be implemented on a regular and sustainable basis.

Keywords Flood hazard · Multi-criteria analysis · GIS · Weighted overlay · Upper Awash River basin · Ethiopia

Introduction

Flooding is a natural part of the hydrological cycle. However, it has the potential to cause death, displacement, and environmental damage, all of which could jeopardize economic progress. Flooding is one of the most common natural disasters, often with disastrous consequences, affecting 170 million people worldwide each year (Kowalzig 2008; Mezgebedingil and Suryabhagavan 2018). Between 1980 and 2010, Ethiopia experienced 86 natural disasters, resulting in the loss of 313,486 human lives, the displacement of 57 million people, and an economic loss of US$ 31.7 million. Flood came in second place among natural disasters, trailing only drought (OFDA 2012).

Floods are among the most shocking natural disasters, according to Rozalis et al. (2010), and can cause irreversible damage. Flooding can occur in a number of different ways. River/stream overflow, heavy rain, breaches in flood protection systems, and rapid melting of ice in the mountains are among the most prominent. With the exception of flash flooding, which occurs only in the foothills, most floods build up over hours to days. River flooding is caused by excessive precipitation and/or melting snow, which causes rivers to overflow their banks and cover territory that is normally not covered by water. Kron (2002) defines formalized.

Flood-inundated areas have been mapped using a combination of geographical information system, remote sensing and multi-criteria decision analysis (MCDA) approaches (Fernández and Lutz 2010; Danumah et al. 2016; Gigovi ç et al. 2017; Samela et al. 2018; Morea and Samanta 2020). Several flood hazard assessment studies have made use of multi-criteria analysis (MCA) techniques. Several researchers (Blistanova et al. 2016; Vojtek and Vojteková 2019;

✉ Tesfa Gebrie Andualem
tesfag23@gmail.com

[1] Irrigation, Drainage and Flood Control Sector, Ethiopian Construction Design and Supervision Works Corporation, Addis Ababa, Ethiopia

[2] Department of Hydraulic and Water Resources Engineering, Debre Tabor University, Debre Tabor, Ethiopia

[3] UniSA-STEM, University of South Australia, Adelaide, Australia

[4] Faculty of Civil and Water Resources Engineering, Bahir Dar Institute of Technology, Bahir Dar, Ethiopia

[5] Department of Environmental and Energy Engineering, Yonsei University, Wonju 26493, Republic of Korea

Desalegn and Mulu 2020; Hussain et al. 2021) examined flood susceptibility zones in Slovakia and Ethiopia using a GIS-based multi-criteria evaluation. Wondim (2016) investigated the flood risk and hazard in Ethiopia's Lower Awash Subbasin. Elsheikh et al. (2015) and Danumah et al. (2016) investigated flood risk in Malaysia and Côte d'Ivoire, respectively. Argaz et al. (2019); Gazi et al. (2019); G.S. Ogato et al. (2020); and Arya and Singh (2021) used GIS-based multi-criteria flood hazard assessment in different parts of the world.

Ethiopia receives the most summer rainfall during the months of June, July, August and September, resulting in devastating floods in some regions of the country (Abebe 2007; Alemu 2015; Getahun and Gebre 2015; Amare and Okubay 2019; Legese and Gumi 2020; Ogato et al. 2020). According to Kefyalew (2003), the most frequently flooded areas in Ethiopia include the Baro-Akobo Basin, the Awash River basin, the Wabi Shebelle, Ribb and Gumara watersheds and the localized flooding risks of Lake Awassa, Lake Besseka and Dire Dawa. The Awash River basin is one of Ethiopia’s major river basins, located in the Rift Valley and prone to flooding (Wondim 2016).

Upper Awash sub basin is a section of the Awash basin that has been impacted by recurring flooding. Flooding has been a major issue in the region, affecting thousands of people and resulting in massive economic losses. Significant floods were reported in the woredas of Sebeta Hawas, Wolmera and Egeria in September 2017, Liben Chukuala and Bora woredas in 2014, 2016 and 2017, at Fentale in 2012, 2015 and 2017, and in 2018 and 2019 at Ilu and Sebeta Hawasa woredas. Flooding has forced thousands of people to flee their homes and sacrificed thousands of animals, particularly in the aforementioned woredas of the upper Awash basin. It also caused massive economic losses and environmental damage. Year after year, infrastructure, health and educational institutions deteriorate; schools in the basin frequently start late due to flooding, and health clinics are closed during the country’s rainy season. Although the downstream area is inundated for days or weeks every year during the rainy season, the Teji River has been flooded for brief periods following severe or prolonged rainfall storms. River flood records in the Teji watershed were recently recorded in the kebeles of Asgori, Teji, Bili, Jigdu Mida, and Tulu Mangora in 2018 and 2019.

Flood hazard mapping and analysis, which identifies the most vulnerable regions based on physical characteristics that indicate the propensity for flooding, is one of the most important parts of early warning systems or methods for the prevention and mitigation of future flood situations. Flood hazard mapping is a critical component of flood-prone land use planning and mitigation strategies (Bhatt et al. 2014). Flood hazard mapping provides easy-to-read charts and maps, allowing planners to identify risk areas and prioritize mitigation activities (Forkuo 2011; Wang et al. 2011; Ajin et al. 2013; Argaz et al. 2019).

The primary objective of this research is to investigate the spatial distribution of flood hazards and to assess potential strategies for protecting the community from displacement and economic loss in the upper Awash subbasin of the Teji watershed. The flood hazard assessment procedure was carried out with this goal in mind, using hazard concepts within an analytic hierarchy process (AHP) framework.

Description of the study area

The Teji watershed is a tributary of the Awash River basin in central Ethiopia, located between 8'23'05"N and 8'50'46"N and 38'7"E and 38'26'30"E, about 60 km from Addis Ababa (Fig. 1). The watershed has a total size of 699.023 km^2. Eutric Vertisols dominate the Teji watershed with an aerial area of 50588.56 ha (72.37%), followed by Chromic Luvisols 10368.2 ha (14.83%), Humic Nitisols 6775.62 ha (9.69%), and Lithic Leptosols covering 2169.9 ha (3.10%). The slope of the watershed ranges from nearly flat to quite steep, and it gradually declines northeastward. A number of minor streams drain the watershed and join to form the Teji River. The elevation of the research area ranges from 2037 to 3575 meters above sea level (m.a.s.l). The research area is divided into three climate zones: Wurch (cold climate with an altitude of more than 3000 m), Dega (highland temperate climate with an altitude of 2500–3000 m), and Woina-Dega (warm climate with an altitude of 1500–2500 m) (NMSA (2001)). Annual rainfall in the watershed ranges from 940 mm in the extreme northeast to 1158 mm in the high hills, with 1027 mm being the average. Cropland, grassland, forest land, shrubland, and built-up area cover (5.17%), (0.52%), (0.38%), and (0.19%) of the study area, respectively.

Materials and methods

Data

Journals, design manuals, books, and other secondary sources were used to collect secondary data. The slope, elevation, drainage density, and proximity to the river of the research region were calculated using the Digital Elevation Model (DEM, 20 * 20 m resolution obtained from SRTM). Soil maps obtained from Ethiopia’s Ministry of Water, Irrigation, and Electricity were used to assess flood risk by evaluating soil type maps. The map of land use was obtained from http://geoportal.rcmd.org. Meteorological (precipitation) data for four selected meteorological stations were obtained from the National Meteorological Agency (NMA): Teji, Tulu bolo, Guranda Meda, and Hombole.

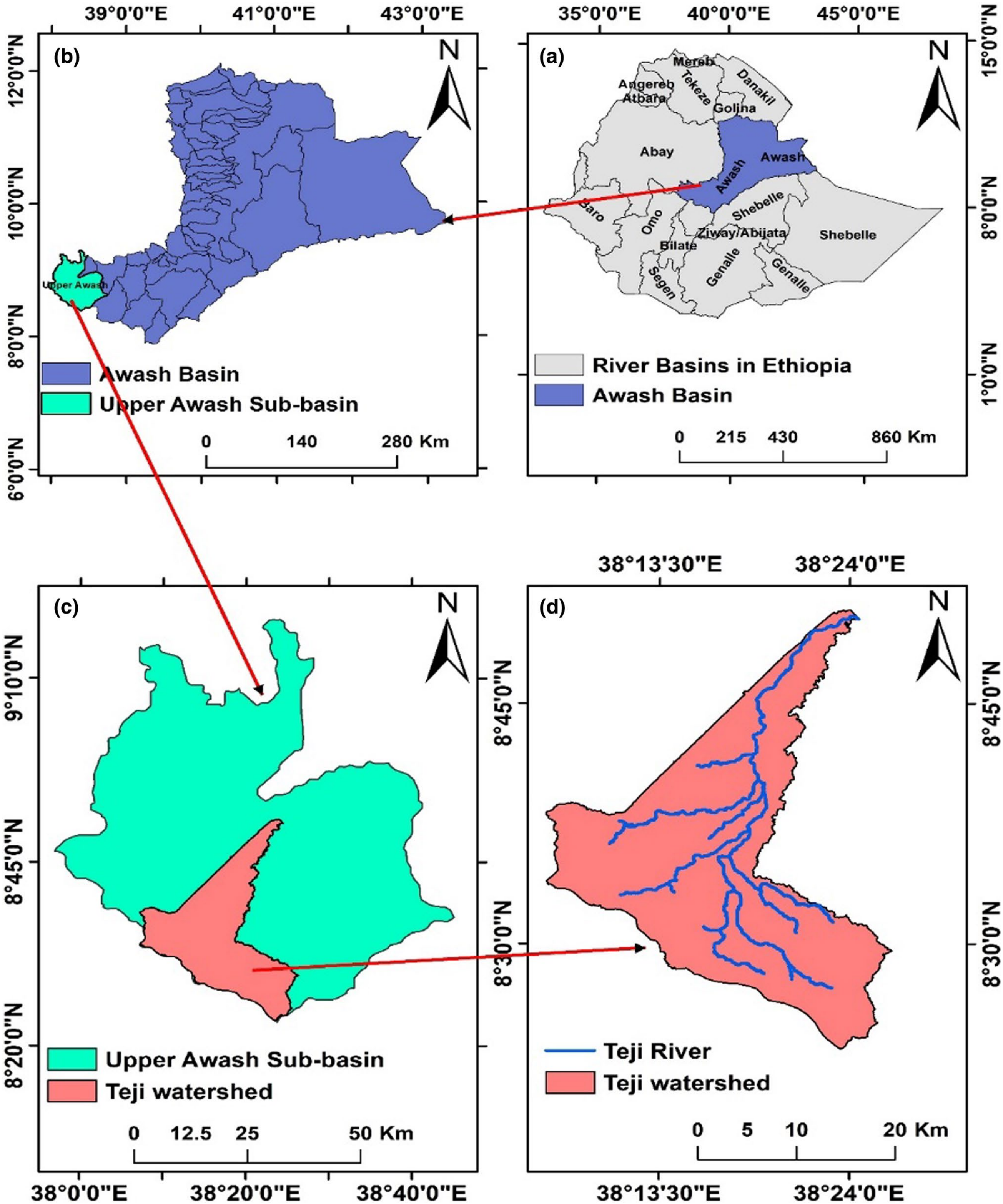

Figure 1 Location of the study area **a** River basins in Ethiopia, **b** Awash river basin, **c** Upper Awash sub-basin and **d** Teji Watershed

Factors that contribute to flood hazard

The major challenge in multi-criteria evaluation (MCE) is determining how to combine information from multiple criteria to generate a single index of assessment. To aid in the processing, data integration and operation of geographical information system (GIS) software, a set of base maps and images were created (Eastman 2001). All preparation procedures, such as downloading, extracting, georeferencing, formatting, and resampling digital data of the factors, were completed prior to analysis. To identify flood-causing variables, field surveys and literature were used. As a result, slope, elevation, drainage density, river proximity, rainfall, soil texture and land use were prioritized in terms of flood hazard relevance (Fig. 2).

Slope factor

The slope is the ratio of a feature's steepness or degree of inclination to the horizontal plane. Slope is an important indicator of flood-prone surface zones (Alemayehu 2007; Wondim 2016). The slope of a slope is an important factor in determining the rate and duration of water flow. Water moves more slowly, collects for a longer period of time, and accumulates on flatter surfaces, making them more vulnerable to flooding than steeper surfaces (Wondim 2016; Gigovi ç et al. 2017; Rimba et al. 2017; Rincón, et al. 2018; Desalegn and Mulu 2020; Singh et al. 2020a). Slope has a significant impact on flood danger assessment because it affects the quantity of surface runoff generated by precipitation, the rate of precipitation, and the flow velocity of water over the equipotential surface. The slope percent map for the research area was created with ArcGIS 10.3.1's spatial analysis tool and a DEM with a resolution of 20 meters (Fig. 3). The research region's slope percentage ranges from

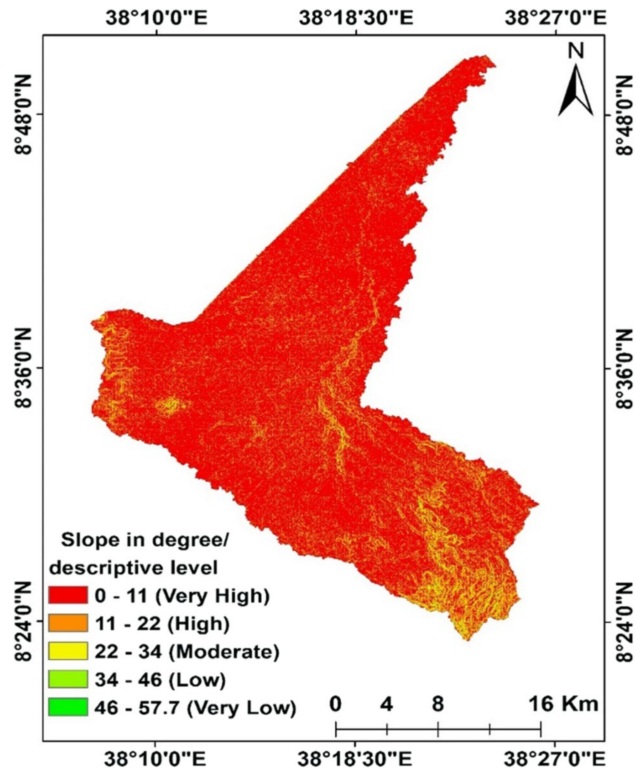

Figure 3 Slope map of the study area

0 to 57.7. Lower slope values represented flatter topography that was especially vulnerable to flooding, whereas higher slope values represented steeper topography that was less vulnerable to flooding. Slopes were categorized into five levels based on their vulnerability to flooding. The slope of the study area was classified into five classes based on its impact on flood risk: extremely high (0–11°), high (11–22°),

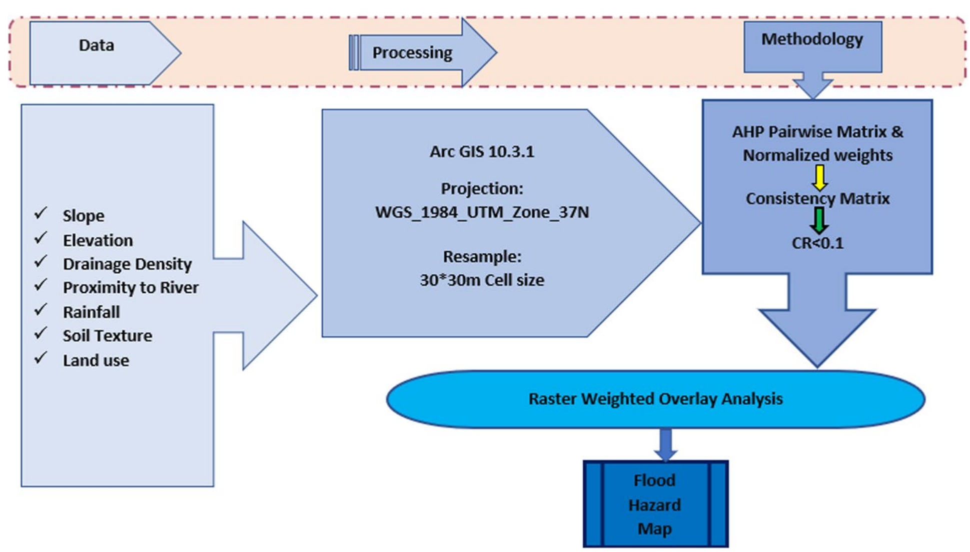

Figure 2 Work flow of flood hazard and risk analysis of teji watershed

moderate (22–34°), low (34–46°) and very low (46–57.7°). Each slope class accounts for about 72, 23.7, 3.5, 0.5 and 0.04% of the total area of the watershed, respectively.

Elevation

The elevation raster layers are created with the help of the ArcGIS environment and the DEM. Using the reclassification tool in the ArcGIS environment, the elevation raster layers were further classified into five groups. Flooding was less of an issue higher elevation, and vice versa (Wondim 2016; Argaz et al. 2019; Choubin, et al. 2019; Gazi, et al. 2019; Ogato, et al. 2020). The elevation of the research area was divided into five categories based on its effect on flood hazard: extremely high (2031–2339 m), high (2339–2648 m), moderate (2648–2957 m), low (2957–3266 m) and very low (3266–3575 m). Each class covers approximately 54.8, 28.3, 8.4, 7.2 and 1.3% of the total area of watershed, respectively (Fig. 4).

Drainage density

The density of drainage is a major factor influencing flood hazard. The drainage system that develops in an area is entirely dependent on the slope, the type of bedrock, and the regional and local fracture pattern (Alemayehu 2007; Wondim 2016). The drainage density is an inverse function of soil permeability. A low permeable surface area is prone to high drainage density, and water from precipitation also leads to high runoff and vice versa. As a result, greater drainage density means that the area is less prone to flooding (Chibssa 2007; Wondim 2016). As a result, as drainage density increases, the rating for drainage density decreases. The technique has been proposed to extract drainage networks from DEMs with a resolution of 20 m using a spatial analysis tool in ArcGIS 10.3.1. Kernel Density was used in a GIS context to determine drainage density area from stream polyline features.

As a result, as drainage density increases, the rating for drainage density decreases. The algorithm has been

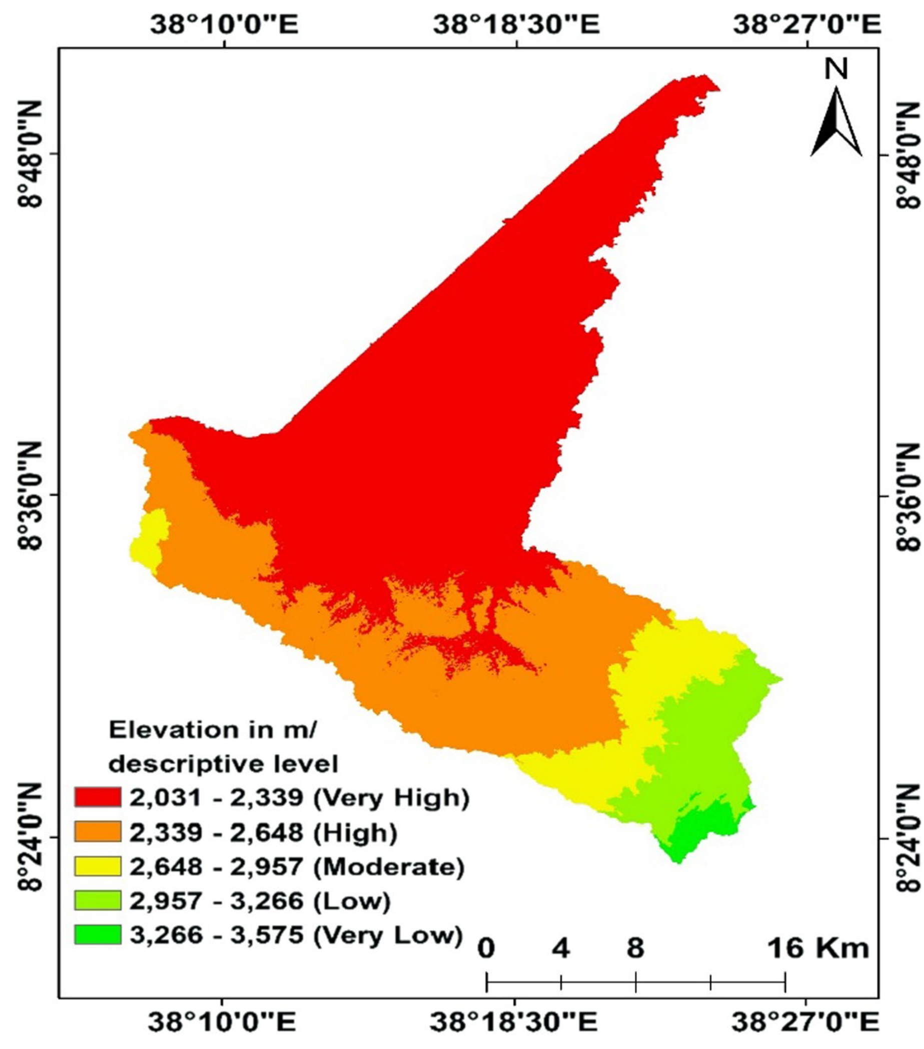

Figure 4 Elevation map of the study area

proposed to extract drainage networks from DEMs with a resolution of 20 m using a spatial analysis tool in ArcGIS 10.3.1. In a GIS environment, Kernel Density was used to calculate drainage density area from stream polyline features (Fig. 5). The drainage density (DD) is calculated by dividing the total length of all streams and rivers in a drainage basin by the drainage basin's total area. As shown in the equation below, drainage density is the total length of the stream segments divided by the unit area (Greenbaum 1985; Magesh et al. 2012; Ouma and Tateishi 2014).

$$\text{Dd} = \frac{\sum_{i=1}^{n} L_i}{A} \quad (1)$$

where $\sum_{i=1}^{n} L_i$ is the total length of drainage in Km, A is total area of study site in Km^2, and n stand for number of drainage networks in the watershed.

Finally, the drainage density was categorized into a continuous scale in accordance with the flood hazard rating. The watershed's drainage density ranges from 0.006 to 8 km/km^2. The class has been divided into five categories based on its effect on flood hazard: extremely high (0.006–2.5 km/km^2), high (2.5–4.5 km/km^{-2}), moderate (4.5–6.0 km/km^2), low (6.0–7.5 km/km^2) and very low (7.5–8.1 km/km^2). Each drainage density class encompasses about 52.2, 37.0, 8.1, 2.3 and 0.5% of the total area of the watershed, respectively.

Proximity to river

One of the primary criteria used to evaluate flood hazard map generation in the study watershed is river proximity. Because river overtopping and flooding in the river buffer zone are the most common cases in the study area (Bapalu and Sinha 2005; Emin Tas 2017; Rincón et al. 2018; Vojtek and Vojteková 2019). This element is critical to include when mapping flood-prone areas in the Teji watershed. In the years 2019 and 2018, there have been reports of flood hazards affecting thousands of people and causing massive economic damage. Despite the fact that the river channel was deep, the river overflowed the bridge and flooded Asgori town during an observation at Asgori town on the Teji river crossing of Reta Desis Bridge. The Teji river is located about 400 m south west of Addis Ababa's main asphalt road to Jima and overflows to the Ilu recreation center. It causes property damage in the Teji town center and beyond. In this study, the class was divided into five categories based on its effect on flood danger, namely extremely high (0–200 m), high (200–400 m), moderate (400–1000 m), low (1000–4700 m) and very low (4700–7680 m) which is derived from the watershed river network (Fig. 6). The proximity map was reclassified and combined with other criterion maps for overlay analysis. Each proximity class accounts for approximately 9.8, 8.6, 21.0, 54.9 and 5.7% of the total watershed area, respectively.

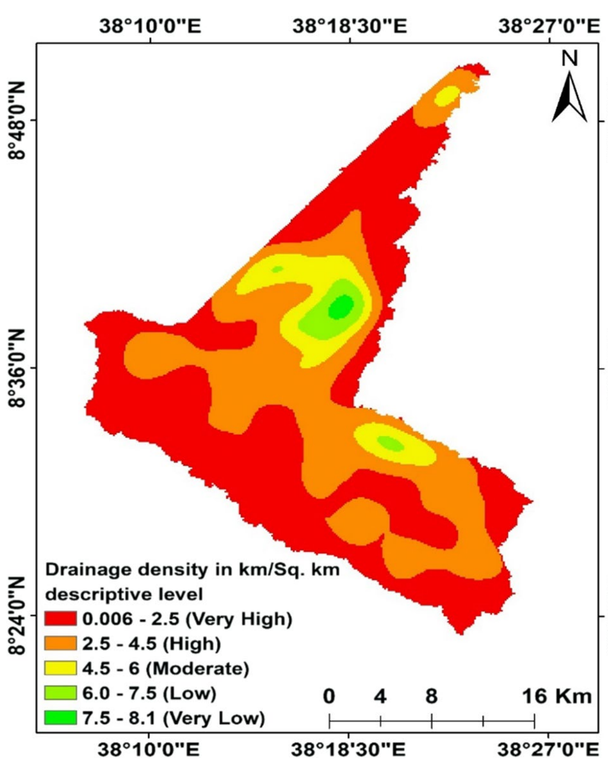

Figure 5 Drainage density map of the study area

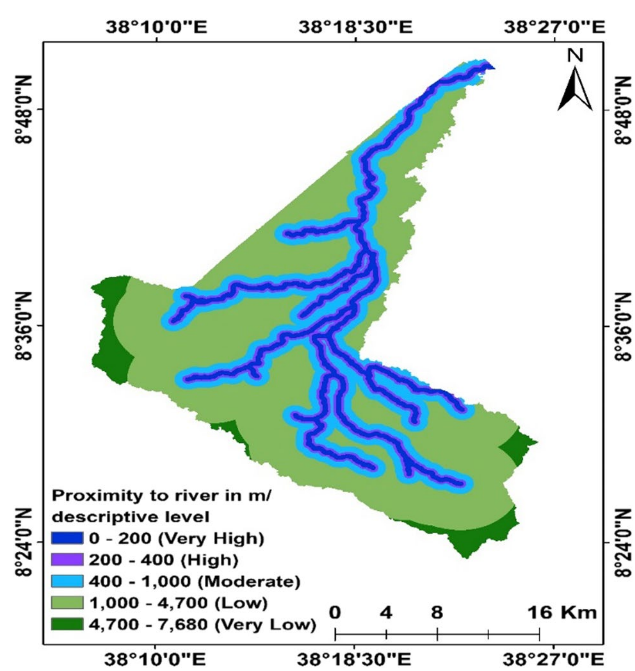

Figure 6 Proximity to River map of the study area

Rainfall

Rainfall is a significant factor in creating a flood danger map. The rainfall map was created using the inverse distance weight method from historical rainfall data collected from meteorological stations located in and around the research area (Ogato et al. 2020; Desalegn and Mulu 2020). The watershed's mean annual rainfall ranges from 940 to 1158 mm, as shown in Fig. 7. Rainfall intensity is important in causing flooding, so weight was assigned to rainfall classes. The greater the amount of rainfall, the greater the flood-producing runoff, and vice versa (Adiat et al. 2012; Blistanova et al. 2016; Gazi et al. 2019). The rainfall in the research area was classified into five categories based on its impact on flood risk: very low (940–983 mm), low (983–1027 mm), moderate (1027–1071 mm), high (1071–1114 mm) and very high (1114–1158 mm). Each rainfall volume class covers about 5.4, 2.8, 22.6, 31.9 and 37.4% of the total area of the watershed, respectively.

Soil texture

The type of soil has a significant impact on the rate of precipitated water infiltration and the water-holding capacity of the area. As a result, it may be considered one of the critical factors in defining flood-prone areas. Sandy soils have higher saturated hydraulic conductivities than finer grained soils due to the greater pore space between the soil particles. The ability of various soil textures to absorb water varies (Wondim 2016). Infiltration, according to Morgan (1995), has a significant impact on the availability and quantity of surface runoff produced by the rainfall-runoff process. As a result, clay soils infiltrate at a much lower rate than sandy soils (Ward and Robinson 1990; Wondim 2016). Soil physical characteristics, particularly soil texture, were considered when developing the soil texture factor. The statistical analysis of soil type reveals that the study area is primarily covered by clay (Eutric Vertisols) soil, accounting for 72.4% area coverage, followed by loam (Chromic Luvisols and Humic Nitisols) and sandy loam (Lithic Leptosols), which account for 24.5 and 3.1% of the total area of watershed (Fig. 8).

Land use/land cover

Land use land cover (LULC) refers to the type of soil deposits and the distribution of built-up areas, cropland, grassland, shrubland and forestland within a given region. The LULC of a watershed play an important role in flood water movement by impeding, delaying or accelerating surface flow. The LULC of the watershed influences infiltration rates, the interaction of surface and groundwater, and debris flow. The study watershed region's land use/land cover was reclassified into five classes based on its ability to increase or decrease the rate of floods. As cities expand in size, impervious cover

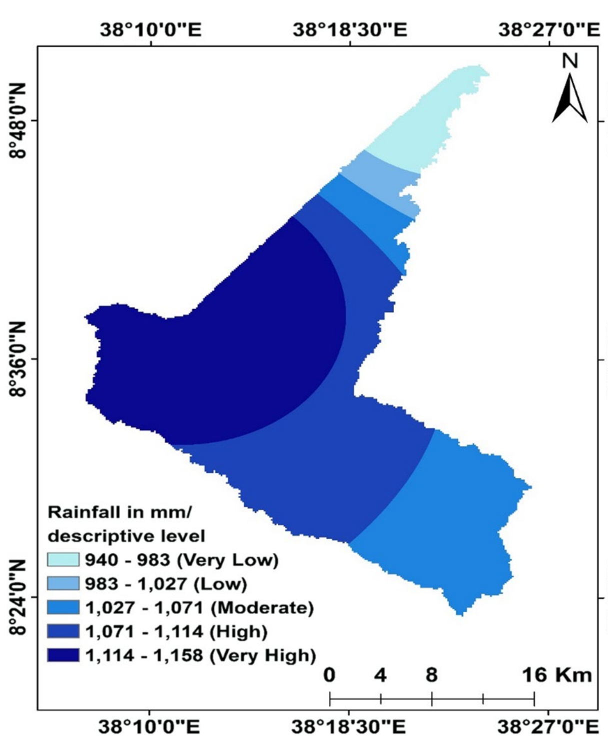

Figure 7 Rainfall distribution map of the study area

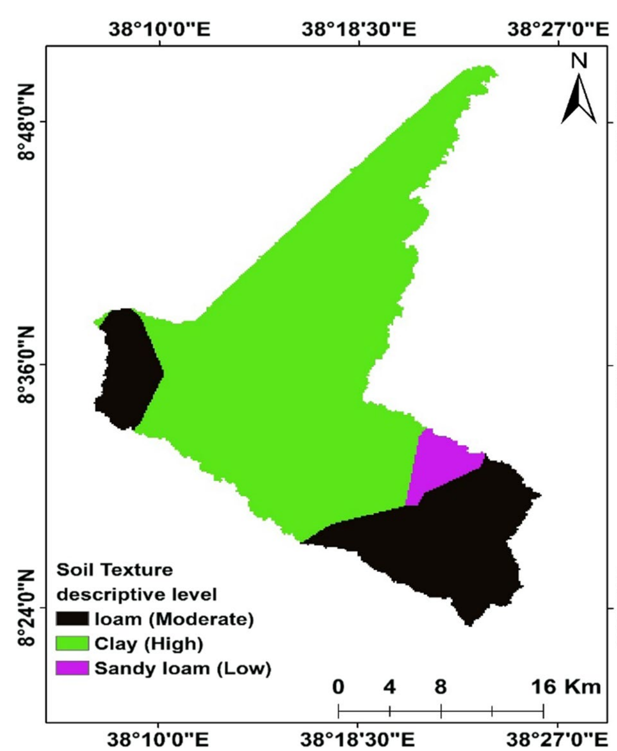

Figure 8 Soil texture map of the study area

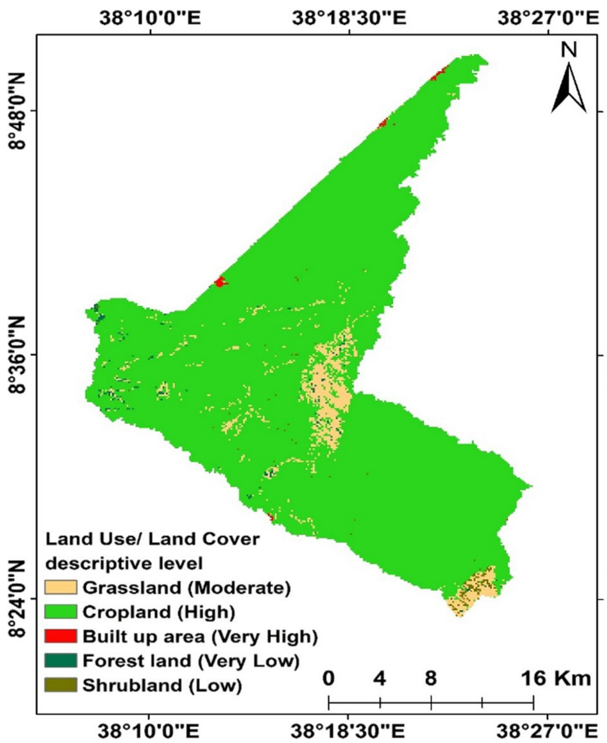

Figure 9 Land use/Land cover map of the study area

increases while forest cover decreases, contributing to an increase in run-off (Tucci 2007; Fura 2013; Blistanova et al. 2016; Wondim 2016; Gazi et al. 2019; Arya & Singh 2021). As a result, built-up areas are classified as extremely high, whereas farmland, grassland and shrubland are classified as high, moderate, and low, respectively. Forestland, on the other hand, has a very low capacity to generate floods and is classified as extremely low, as seen in (Fig. 9). Cropland accounts for 93.7% of the land use in the research region, whereas built-up, grassland, shrubland, and forestland areas account for 0.2, 5.2, 0.4 and 0.5%, respectively.

AHP methodology

In AHP, weights (Table 2, Table 3) and thematic layers of each level (criteria classes) are assigned and their relative importance is determined using Saaty's 1–9 scale. The relevance or preference of each thematic layer relative to the other thematic layers on flood prone area delineation selection was conveyed by assigning weights. This was accomplished by utilizing related review literatures, field observation, and expert judgment to populate a pairwise comparison matrix from which a set of weights known as Eigenvectors, as well as consistency ratios, were generated for each of

Table 1 Satty's scale of relative importance (Saaty 1980; Saaty and Vargas 1991)

Intensity of importance	Degree of preference	Explanation
1	Equal importance	Two activities contribute equally to the objective
3	Moderate importance of one factor over another	Experience and judgment slightly favor one activity over another
5	Strong or essential importance	Experience and judgment strongly favor one activity over another
7	Very strong importance	An activity is strongly favored and its dominance demonstrated in practice
9	Extreme importance	The evidence favoring one activity over another is of the highest possible order of affirmation
2,4,6,8	Intermediate values between two adjacent judgments	When compromise is needed

Table 2 Pairwise comparison of seven criterion matrix

Factor	Slope	Elevation	Drainage density	Proximity to river	Rainfall	Soil texture	Land use
Slope	1						
Elevation	1/2	1					
Drainage density	1/3	1/2	1				
Proximity to river	1/3	1/3	1/2	1			
Rainfall	1/5	1/5	1/3	1/3	1		
Soil texture	1/7	1/7	1/5	1/5	1/3	1	
Land use	1/9	1/9	1/7	1/7	1/5	1/3	1

Table 3 Pairwise comparison of seven criterion decimal matrix

Factor	Slope	Elevation	Drainage density	Proximity to river	Rainfall	Soil texture	Land use
Slope	1.00	2.00	3.00	3.00	5.00	7.00	9.00
Elevation	0.50	1.00	2.00	3.00	5.00	7.00	9.00
Drainage density	0.33	0.50	1.00	2.00	3.00	5.00	7.00
Proximity to river	0.33	0.33	0.50	1.00	3.00	5.00	7.00
Rainfall	0.20	0.20	0.33	0.33	1.00	3.00	5.00
Soil texture	0.14	0.14	0.20	0.20	0.20	1.00	3.00
Land use	0.11	0.11	0.14	0.14	0.14	0.20	1.00
Sum	2.62	4.29	7.18	9.68	17.34	28.20	41.00

the criteria under consideration (Wondim 2016; Ogato et al. 2020; Arya and Singh 2021). Flood hazard factors are rated on a scale of 1 to 9, with 1 indicating that both elements are equally important and 9 indicating that one component is more important than the other. The reciprocal of 1 to 9 (1/1 and 1/9) denotes that one is less important than the other (Saaty 1980; Saaty and Vargas 1991). The factor weights were evaluated in order to conduct a multi-criteria assessment of the effect on flood generation in a study area. The following are the fundamental procedures for determining the indicator's weight and consistency ratio (CR) (Tables 1, 2, 3, and 4):

Step 1. Establishment of judgment matrices (*P*) by pairwise comparison.

$$P = \begin{pmatrix} P_{11} & P_{12} & \cdots & P_{1n} \\ P_{21} & P_{22} & \cdots & P_{2n} \\ \vdots & \cdots & \ddots & \vdots \\ P_{n1} & P_{n2} & \cdots & P_{mn} \end{pmatrix} \quad (2)$$

Where, *n* denote the *n*th row and m denotes the *m*th column elements of the judgment matrix.

Step 2. Calculation of normalized weight

This step is to normalize the matrix by totaling the numbers in each column. Each entry in the column is then divided by the column sum to yield its normalized score. The sum of each column is 1.

$$W_n = \left(\mathrm{GM}_n \Big/ \sum_{n=1}^{ni} \mathrm{GM}_n\right) \quad (3)$$

Where, the geometric mean of the *i*th row of the judgement matrices is calculated as:

$$\mathrm{GM}_n = \sqrt[ni]{P_{1n} P_{2n} \cdots P_{\mathrm{mn}_i}} \quad (4)$$

Step 3. Calculates a consistency ratio (CR) to verify the coherence of the judgements. Now, calculate the consistency ratio and check its value. The purpose for doing this is to make sure that the original preference ratings were consistent (Table 8).

$$\mathrm{CR} = \frac{\mathrm{CI}}{\mathrm{RI}} \quad (5)$$

Consistency index (CI) is denoted as follows:

$$\mathrm{CI} = \frac{\lambda_{\max} - n_i}{n_i - 1} \quad (6)$$

Max is the eigenvalue of judgment matrix and it is calculated as:

$$\lambda_{\max} = \sum_{n=1}^{n_i} \frac{(\mathrm{PW})_n}{n_i w_n} \quad (7)$$

Where, *W* is the weight vector (column). Random index (RI) can be obtained from standard tables (Table 7, Saaty 1980).

Table 4 Normalized pairwise matrix calculated

Factor	Slope	Elevation	Drainage density	Proximity to river	Rainfall	Soil texture	Land use
Slope	0.38	0.47	0.42	0.31	0.29	0.25	0.22
Elevation	0.19	0.23	0.28	0.31	0.29	0.25	0.22
Drainage density	0.13	0.12	0.14	0.21	0.17	0.18	0.17
Proximity to river	0.13	0.08	0.07	0.10	0.17	0.18	0.17
Rainfall	0.08	0.05	0.05	0.03	0.06	0.11	0.12
Soil texture	0.05	0.03	0.03	0.02	0.01	0.04	0.07
Land use	0.04	0.03	0.02	0.01	0.01	0.01	0.02

Table 5 Determined relative criterion weights

Factor	slope	Elevation	Drainage density	Proximity to river	Rainfall	Soil texture	Land use	Criteria weight
Slope	0.38	0.47	0.42	0.31	0.29	0.25	0.22	0.33
Elevation	0.19	0.23	0.28	0.31	0.29	0.25	0.22	0.25
Drainage density	0.13	0.12	0.14	0.21	0.17	0.18	0.17	0.16
Proximity to river	0.13	0.08	0.07	0.10	0.17	0.18	0.17	0.13
Rainfall	0.08	0.05	0.05	0.03	0.06	0.11	0.12	0.07
Soil texture	0.05	0.03	0.03	0.02	0.01	0.04	0.07	0.04
Land use	0.04	0.03	0.02	0.01	0.01	0.01	0.02	0.02

Table 6 The Eigen vector weights of each flood factors obtained after the pairwise comparison

Factors	Normalized weight	Influence (%)
Slope	0.33	33.3
Elevation	0.25	25.3
Drainage density	0.16	15.9
Proximity to river	0.13	12.8
Rainfall	0.07	7.0
Soil texture	0.04	3.7
Land use	0.02	2.0
Sum	1.00	100

In practice, a CR of 0.1 or below is considered acceptable. Any higher value at any level indicates that the judgments warrant re-examination.

In this study, seven factors (slope, elevation, drainage density, proximity to river, rainfall, soil texture and land use) were used to delineate flood prone zones. The impact of these factors on flood-prone area delineation is not the same. The weight of each factor was assigned based on its influence on the amount, flow velocity and other criteria related to rainfall-runoff, as well as references to literature (Elsheikh et al. 2015; Danumah et al. 2016; Blistanova et al. 2016; Wondim 2016; Argaz et al. 2019; Gazi et al. 2019; Vojtek and Vojteková 2019; Hussain et al. 2021) (Table 5).

A factor's weight value indicates the proportion of its value in flood hazard prone area zonation, with the dominant influencing factor receiving a high weight value (Table 6 and Table 9). Slope, for example, has a score weight of 33.3%, followed by elevation, rainfall, drainage density, proximity to river, soil texture and land use, which all have score weights of 25.3, 15.9, 12.8, 7.0, 3.7 and 2.0%, respectively (Table 6).

Multi-Criteria Evaluation of flood hazard

A multi-criteria decision-making approach known as the AHP was used to determine the rankings and weights of the sub-factors and map layer based on their level of effect on the result. These layers were then subjected to a weighted overlay analysis, and the final resultant map was generated and classified based on the flood hazard model's indication of their influence on flood danger (Eq. 9). In general, the flowchart depicted the study process (Fig. 2) (Table 8).

$$\text{Flood hazard} = \sum W_i X_i \tag{8}$$

Where W_i = weight of factor i; X_i = criterion score of factors i.

Then in case of this study the final flood hazard map was determined using Eq. below.

$$\begin{aligned}\text{Flood hazard} =\,& 0.337 \times (\text{Slope}) + 0.253 \times (\text{Elevation}) \\ & + 0.159 \times (\text{Drainage density}) + 0.128 \\ & \times (\text{Proximity to river}) + 0.07 \times (\text{Rainfall}) \\ & + 0.037 \times (\text{Soil texture}) \\ & + 0.02 \times (\text{Land use})........9\end{aligned} \tag{9}$$

Result and discussions

Flood hazard mapping

The flooding hazard in the Teji watershed revealed that 2781.09 ha (3.98%), 14337.77 ha (20.51%), 13384.69 ha (19.15%), 30251.89 ha (43.28%), and 9146.85 ha (13.09%) were accordingly categorized to very low, low, moderate, high and very high flood susceptibility (Fig. 11). High to extremely high danger zones are primarily concentrated

Table 7 Random inconsistency indices

n	1	2	3	4	5	6	7	8	9	10
RI	0.00	0.00	0.58	0.90	1.12	1.24	1.32	1.41	1.46	1.49

Table 8 Determined consistency ratios (CR)

Factor	Slope	Elevation	Drainage density	Proximity to river	Rainfall	Soil texture	Land use	Weighted sum value	Criteria weight	Weighted sum/ weighted criteria
Slope	0.38	0.47	0.42	0.31	0.29	0.25	0.22	2.33	0.33	7.47
Elevation	0.19	0.23	0.28	0.31	0.29	0.25	0.22	1.77	0.25	7.57
Drainage density	0.13	0.12	0.14	0.21	0.17	0.18	0.17	1.11	0.16	7.49
Proximity to river	0.13	0.08	0.07	0.10	0.17	0.18	0.17	0.90	0.13	7.31
Rainfall	0.08	0.05	0.05	0.03	0.06	0.11	0.12	0.49	0.07	7.07
Soil texture	0.05	0.03	0.03	0.02	0.01	0.04	0.07	0.26	0.04	6.90
Land use	0.04	0.03	0.02	0.01	0.01	0.01	0.02	0.14	0.02	7.05
Total	1.00	1.00	1.00	1.00	1.00	1.00	1.00		CI	0.044
									RI	1.320
									CR	0.034
									CR<0.1 Consistency is acceptable	

in the watershed's center and lower reaches. These high to very high flood hazard zone regions are distinguished by flat areas with low slope gradient, lower elevation, low drainage density and proximity to the river, all of which are significant conditioning variables for flood hazard mapping. There were extremely low to low flood danger zones, which were primarily located along the upstream section of the watershed and were distinguished by their steep slope, higher elevation, and low drainage density (Figs. 10and 11). This finding is similar to that of a flood vulnerability study conducted at Ethiopia's Lower Awash Sub-basin (Wondim 2016); the Souss Watershed in middle western Morocco by Argaz et al. (2019); the northeastern part of Bangladesh by Gazi et al. (2019); the Fetam watershed in Ethiopia's upper Abbay basin by Desalegn and Mulu (2020); and the Ghaghara River basin in Uttar Pradesh (2021) (Table 9).

According to the findings of the spatial study, Illu and Becho woredas or districts are more vulnerable to very high flood risk (Table 10). This suggested that careful flood management and mitigation measures should be implemented first in these districts, before moving on to other districts. In contrast, the Kersana Malima district is less vulnerable to high and very high floods.

Validation of the flood hazard map

Model validation is the process of systematically comparing model outputs to independent real-world observations in order to assess quantitative and qualitative concordance with reality. Many models are used by researchers to assess flood susceptibility in various parts of the world, but it is critical to test the model's outputs to ensure that the model adequately represents the actual ground conditions or recorded observations. By comparing model output to observable data, model calibration and validation can be accomplished.

To validate the Teji watershed flood hazard map results, the locations of historical flood occurrences were created using a field visit to collect flood markings and an interview with Teji watershed locals, who provided relevant data on 26 flooding sites (Fig. 12). These historical flood spots were superimposed on the model's output. The watershed's flooding history reveals that flash floods affect flat sloping regions such as much of the Ilu, Becho, Weliso, and some sections of other Woredas, whereas river flooding affects Teji town, Asgori town, as well as Bili, Jigdu Meda and Tulu Mangora Kebeles. Fig. 13 shows photographs taken in and around Teji and Asgori towns to depict flood marks for the 2019 flood event as well as flash flooded regions in Teji town in 2021. All historical flood points gathered, according to the predicted output, are located in the high and very high flood susceptibility zones, indicating the reliability of the flood vulnerability model used in this study.

Conclusion

Floods have disrupted people's lives, as well as social and environmental assets. Flood simulation and risk assessments are strategic planning tools for effectively reducing flood risk and damage, despite the fact that they cannot be avoided. A flood management strategy must include the assessment of flood hazard areas. The proposed method was used to identify flood-prone areas in Ethiopia's Teji watershed and upper Awash River basin. Many studies have used multi-criteria evaluation methods, which have proven to be an extremely effective tool in assisting decision-making processes. The seven distinct input maps that were created were slope, elevation, drainage density, river proximity, rainfall, soil texture and land use. Finally, the simulated result maps, such as floods, are presented. The obtained results were validated

Table 9 AHP rank and weights for the parameters of flood hazard for Teji watershed

Factors	Average weights	Sub-factors	Ranking	Normalized weight	Area %
Slope (°)	0.33	0–11	1	0.50	72.25
		11–22	2	0.26	23.67
		22–34	3	0.13	3.51
		34–46	4	0.07	0.53
		46–57.7	5	0.03	0.04
Elevation (m)	0.25	2031–2339	1	0.42	54.81
		2339–2648	2	0.26	28.27
		2648–2957	3	0.16	8.41
		2957–3266	4	0.10	7.27
		3266–3575	5	0.06	1.24
Drainage density (km km^{-2})	0.16	0.006–2.5	1	0.46	52.22
		2.5–4.5	2	0.27	36.95
		4.5–6	3	0.15	8.05
		6–7.5	4	0.08	2.34
		7.5–8.1	5	0.04	0.45
Proximity to river (m)	0.13	0–200	1	0.57	9.84
		200–400	2	0.21	8.55
		400–1000	3	0.12	20.99
		1000–4700	4	0.06	54.85
		4700–7680	5	0.03	5.77
Rainfall (mm)	0.07	940–983	5	0.04	5.42
		983–1027	4	0.07	2.77
		1027–1071	3	0.13	22.55
		1071–1114	2	0.26	31.91
		1114–1158	1	0.50	37.35
Soil texture	0.04	Clay	1	0.63	72.40
		loam	2	0.26	24.51
		Sandy loam	3	0.11	3.09
Land use/Land cover	0.02	Built up area	1	0.50	0.19
		Cropland	2	0.26	93.74
		Grassland	3	0.13	5.17
		Shrubland	4	0.07	0.38
		Forest land	5	0.03	0.52

against data from previous floods in the watershed's ground truth points of observed flood affected areas (hazard map, validation map). The collected data were analyzed using the analytic hierarchy method and mapped using geographic information system techniques, resulting in a land suitability map. According to the flood hazard model output, 4.0, 20.5, 19.2, 43.3 and 13.1% of land are at risk of flooding, with very low, low, moderate, high, and very high flood dangers, respectively. Remote sensing and GIS techniques have been shown to be extremely useful in detecting flood risk zones and developing flood susceptibility maps. It has also been demonstrated that the multi-criteria analysis technique

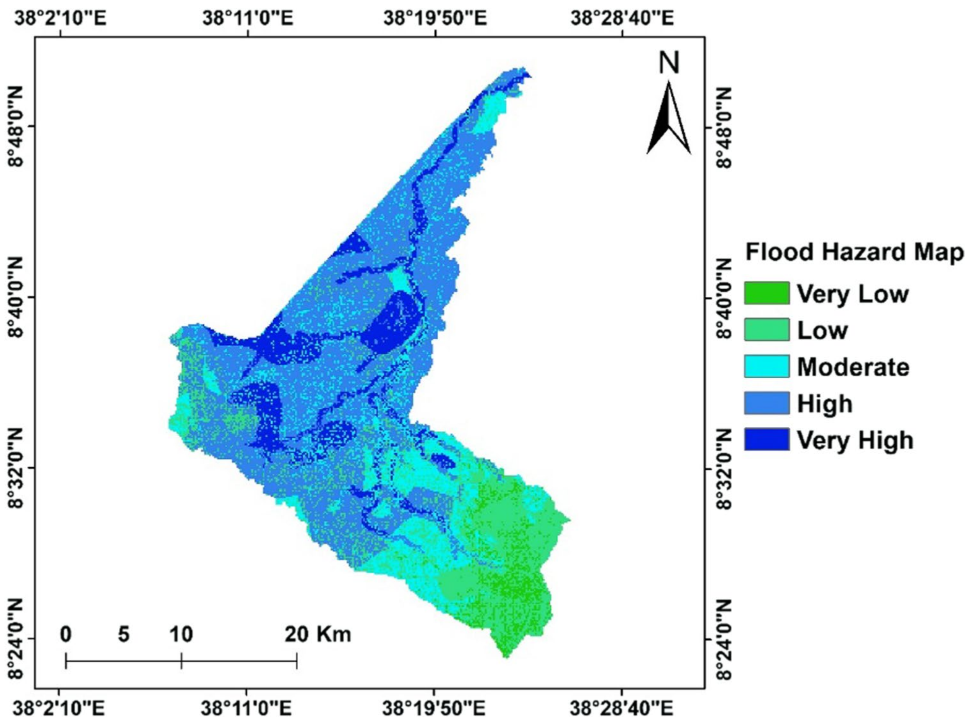

Figure 10 Flood Hazard Map of Teji Watershed

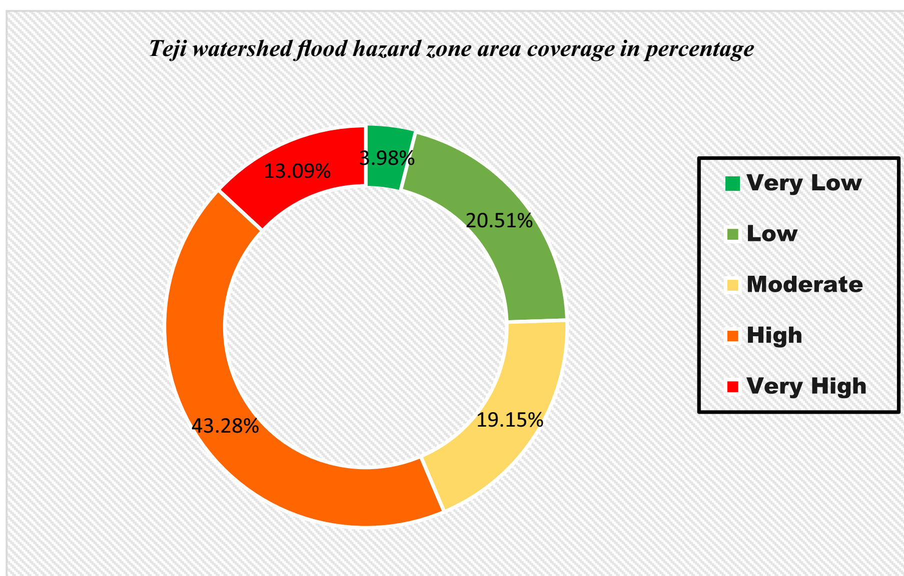

Figure 11 Pie chart shows the Teji watershed flood hazard zone area coverage in %age.

Table 10 Flood hazard zones coverage by Woreda and Kebele

Woreda	Kebele	Very Low		Low		Moderate		High		Very High	
		Area in ha	Area (%)	Area in ha	Area (%)	Area in ha	Area (%)	Area in ha	Area (%)	Area in ha	Area (%)
Ilu	Teji town	0.0	0.0	16.3	22.9	2.3	3.2	38.3	53.9	14.2	20.0
	Asigori town	0.0	0.0	1.2	2.0	23.1	38.7	35.3	59.3	0.0	0.0
	Jigdu Mida	0.0	0.0	54.9	9.1	114.0	19.0	287.9	47.9	144.1	24.0
	Alengo Tulu	0.0	0.0	5.9	17.3	4.1	12.2	6.4	18.9	17.4	51.5
	Buti Teglo	0.0	0.0	8.5	7.6	27.9	24.9	46.6	41.6	29.0	25.9
	Bili	0.0	0.0	135.4	15.8	424.9	49.6	208.9	24.4	87.5	10.2
	Tulu Mangora	0.0	0.0	0.0	0.0	0.0	0.0	5.5	100.0	0.0	0.0
	Weserbi Nado	0.0	0.0	0.0	0.0	3.0	2.7	107.5	97.3	0.0	0.0
	Weserbi Besi	0.0	0.0	25.6	1.8	265.3	18.3	983.7	68.0	172.7	11.9
	Keta	0.0	0.0	15.2	2.8	155.1	28.1	381.2	69.1	0.0	0.0
Becho	Tulu Bolo town	0.0	0.0	2.8	1.5	46.7	25.5	115.9	63.3	17.7	9.7
	Awase Bune	0.0	0.0	72.2	3.2	304.0	13.4	1502.2	66.4	385.1	17.0
	Jato	0.0	0.0	23.1	0.9	451.3	17.8	1738.5	68.6	322.5	12.7
	Wesrebi Abiti	0.0	0.0	0.0	0.0	101.5	15.4	506.3	77.1	49.1	7.5
	Wesrebi Paa	0.0	0.0	0.0	0.0	25.1	22.0	89.0	78.0	0.0	0.0
	Basa	0.0	0.0	41.4	4.1	239.7	23.8	567.0	56.4	157.4	15.7
	Senbero Terewo	0.0	0.0	247.4	7.9	262.0	8.4	1702.1	54.6	905.2	29.0
	Qobo	0.0	0.0	21.7	4.5	53.2	11.1	322.4	67.3	81.7	17.1
	Soyema	0.0	0.0	3.2	0.3	69.5	7.1	336.2	34.2	574.8	58.4
	Batu Cherecha	0.0	0.0	117.6	13.1	104.6	11.6	667.9	74.2	10.3	1.1
	Kata Eniselale	0.0	0.0	45.2	2.0	420.2	18.9	1165.2	52.5	587.5	26.5
	Soda Lebene	0.0	0.0	196.1	5.5	417.0	11.8	1481.0	41.8	1444.7	40.8
	Ourago Tede	0.0	0.0	71.3	4.8	345.9	23.5	839.8	57.0	215.3	14.6
	Bebele Debenya	0.0	0.0	9.6	0.5	410.2	19.8	1249.9	60.3	402.6	19.4
	Bogi Gefere	0.0	0.0	198.6	8.8	387.6	17.1	811.8	35.8	871.5	38.4
	Mende Tufesa	0.0	0.0	977.0	31.2	416.6	13.3	1640.3	52.4	94.3	3.0
	Shankur Tereqo	0.0	0.0	872.3	25.9	301.3	8.9	1614.1	47.9	579.4	17.2
Weliso	Deyo Kora	0.0	0.0	70.4	60.0	13.0	11.1	33.9	28.9	0.0	0.0
	Sonbota Yabata	0.0	0.0	267.2	49.2	205.9	37.9	70.0	12.9	0.0	0.0
	Beda Kero	0.0	0.0	11.0	50.6	0.0	0.0	10.7	49.4	0.0	0.0
	Gadu Kistana	0.0	0.0	6.1	94.5	0.0	0.0	0.4	5.5	0.0	0.0

Table 10 (continued)

Woreda	Kebele	Very Low		Low		Moderate		High		Very High	
		Area in ha	Area (%)	Area in ha	Area (%)	Area in ha	Area (%)	Area in ha	Area (%)	Area in ha	Area (%)
Seden Sodo	Herbu town	0.0	0.0	14.3	25.1	3.6	6.3	39.2	68.6	0.0	0.0
	Aebisa leku gidawa	0.0	0.0	310.7	24.6	94.0	7.4	800.7	63.4	58.1	4.6
	Mudana Aebaye	0.0	0.0	618.1	21.1	670.7	22.9	1223.4	41.8	416.7	14.2
	Aurago Kelcha	0.0	0.0	301.6	10.2	654.8	22.1	1281.9	43.4	718.5	24.3
	Alga Weserbi	28.7	0.9	830.2	26.5	1248.8	39.9	795.6	25.4	229.8	7.3
	Tolo dalota	30.0	2.5	366.8	30.2	311.2	25.6	447.1	36.8	61.0	5.0
	Tole Balekasi	0.0	0.0	576.5	28.0	207.1	10.1	1255.6	61.0	20.5	1.0
	Adadi Borele	0.0	0.0	60.9	29.3	101.2	48.7	45.8	22.0	0.0	0.0
	Gidano Dalota	4.5	0.5	364.4	40.4	401.2	44.5	131.5	14.6	0.0	0.0
	Fisawa Chewaketero	176.6	16.2	498.4	45.8	413.8	38.0	0.0	0.0	0.0	0.0
	Gude Dula Yabeta	1246.3	34.4	1383.0	38.2	855.6	23.6	137.7	3.8	1.0	0.0
	Ejoy Eskedey	158.5	64.5	87.2	35.5	0.0	0.0	0.0	0.0	0.0	0.0
Kersana Malima	Cheleba titu	6.1	3.3	175.7	95.7	1.9	1.0	0.0	0.0	0.0	0.0
	Awa dergego	480.5	27.0	1201.9	67.5	81.9	4.6	16.3	0.9	0.0	0.0
	Awawayu	1140.8	46.2	1187.5	48.1	130.2	5.3	12.7	0.5	0.0	0.0
	Ilalewaqo	740.6	69.3	328.4	30.7	0.0	0.0	0.0	0.0	0.0	0.0
	Deweldera	247.1	45.1	300.7	54.9	0.0	0.0	0.0	0.0	0.0	0.0
Tole	Migirdi Wesarbi	0.0	0.0	13.3	2.6	35.4	6.8	432.2	83.7	35.5	6.9
	Lutaji	0.0	0.0	25.4	6.7	31.6	8.3	301.0	79.4	21.3	5.6
	kersiti Areda	0.0	0.0	20.4	3.3	97.8	15.8	455.4	73.7	44.4	7.2
	Malima na Tumechirfa	0.0	0.0	8.4	48.3	5.0	28.5	4.0	23.1	0.0	0.0
	Maliman Soden Botene	275.4	14.8	1241.8	67.0	285.9	15.4	51.7	2.8	0.0	0.0
	Tume Wayu	107.0	6.6	519.3	31.8	658.6	40.3	174.3	10.7	173.1	10.6
	Gonan na Bobisa	0.0	0.0	669.0	23.9	1227.0	43.8	677.8	24.2	226.9	8.1
	Armufo Teji	0.0	0.0	70.4	4.7	425.7	28.3	841.2	55.9	168.5	11.2

Figure 12 Distribution of Ground Truth Points of Observed Flood Affected Areas in 2019 and Administrative Kebeles

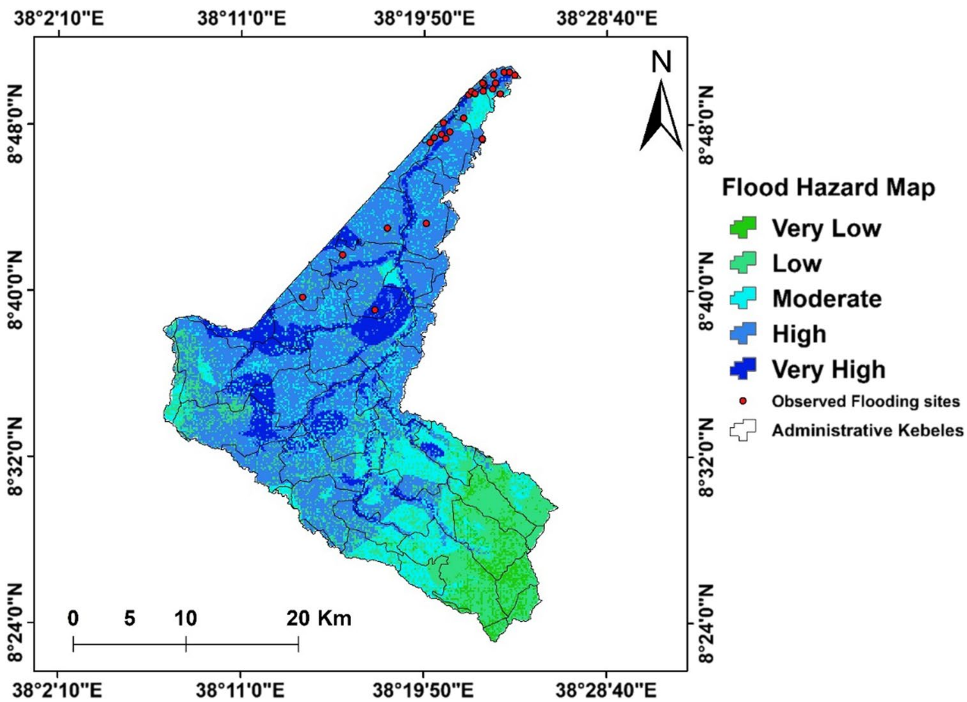

Figure 13 Flood marks of 2019 river flood event in (**a**), (**c**) in Teji and (**b**) in Asgori towns, and (**d**, **e**, **f**) flash flood on Teji town around Ilu Police station and Hidasie Telecom 2021

may be useful in assisting local governments and government agencies in properly identifying flood-prone areas and assisting in the implementation of appropriate flood control strategies in such areas.

Funding The authors received no direct funding for this research.

Declarations

Conflict of interest The authors declare no competing interests.

References

Abebe F (2007) Flood Hazard Assessment Using GIS in Becho Plain, Upper Awash Valley, South West of Addis Ababa. Addis Ababa. Unpublished MSc Thesis, Addis Ababa University, Addis Ababa, Ethiopia

Adiat KAN, Nawawi MNM, Abdullah K (2012) Assessing the accuracy of GIS-based elementary multi criteria decision analysis as a spatial prediction tool—A case of predicting potential zones of sustainable groundwater resources. J Hydrol 440–441:75–89

Ajin RS, Krishnamurthy RR, Jayaprakash M, Vinod PG (2013) Flood hazard assessment of Vamanapuram River basin, Kerala, India: an approach using remote sensing & GIS techniques. Adv Appl Sci Res 4(3):263–274

Alemayehu Z (2007) Modeling of Flood hazard management for forecasting and emergency response of 'Koka' area within Awash River basin using remote sensing and GIS method. Unpublished Msc Thesis, Addis Ababa University, Ethiopia

Alemu YT (2015) Flash flood hazard in Dire Dawa, Ethiopia. J Soc Sci Humanit 1(4):400–414

Amare GN, Okubay GA (2019) Flood hazard risk vulnerability mapping using Geo-spatial and MCDA around Adigrat, Tigray Region, Northern Ethiopia. Momona Ethiopian J Sci 7(1):90–107

Argaz A, Ouahman B, Darkaoui A, Bikhtar H, Ayouch E, Lazaar R (2019) Flood hazard mapping using remote sensing and GIS Tools: a case study of souss watershed. J Mater Environ Sci 10(2):170–181

Arya AK, Singh AP (2021) Multi criteria analysis for flood hazard mapping using GIS techniques: a case study of Ghaghara River basin in Uttar Pradesh, India. Arab J Geosci 14(8):1–12

Bapalu GV, Sinha R (2005) GIS in flood hazard mapping: a case study of Kosi River Basin, India. GIS Dev Weekly 1(13):1–3

Bhatt GD, Sinha K, Deka PK, Kumar A (2014) Flood hazard and risk assessment in Chamoli District, Uttarakhand using satellite remote sensing and GIS techniques. Int J Innov Res Sci Eng Technol 3(8):9

Blistanova M, Zeleňáková M, Blistan P, Ferencz V (2016) Assessment of flood vulnerability in Bodva river basin Slovakia. Acta Montanistica Slovakia 21(1):19–28

Chibssa AF (2007) Flood hazard assessment using GIS in Bacho Plain, Upper Awash Valley, South west of Addis Ababa. Master of Science Thesis. Addis Ababa University, Addis Ababa

Choubin B, Moradi E, Golshan M, Adamowski J, Sajedi-Hosseini F, Mosavi A (2019) An ensemble prediction of flood susceptibility using multivariate discriminant analysis, classification and regression trees, and support vector machines. Sci Total Environ 2019(651):2087–2096

Danumah JH, Odai SN, Saley BM et al (2016) Flood risk assessment and mapping in Abidjan district using multi-criteria analysis (AHP) model and geoinformation techniques, (cote d'ivoire). Geoenviron Disasters 3:10

Desalegn H, Mulu A (2020) Flood vulnerability assessment using GIS at Fetam watershed, upper Abbay basin, Ethiopia. Heliyon. https://doi.org/10.1016/j.heliyon.2020.e05865

Eastman JR (2001) Guide to GIS and image processing volume. Clark University USA

Elsheikh RFA, Ouerghi S, Elhag AR (2015) Flood risk map based on GIS, and multi criteria techniques (case study Terengganu Malaysia). J Geograph Inf Syst 7:348–357. https://doi.org/10.4236/jgis.2015.74027

Fernández D, Lutz M (2010) Urban flood hazard zoning in Tucumán Province, Argentina, using GIS and multicriteria decision analysis. Eng Geol. 111:90–98

Forkuo EK (2011) Flood hazard mapping using aster image data with GIS. Int J Geomat Geosci 1(4):19

Fura GD (2013) Analyzing and modeling urban land cover change for run-off modeling in Kampala, Uganda. Thesis of master of science. University of Twente, Enschede, The Netherlands

Gazi Y, Islam A, Hossai S (2019) Flood-hazard mapping in a regional scale-way forward to the future hazard Atlas in Bangladesh. Malaysian J Geosci 3(1):01–11

Getahun YS, Gebre SL (2015) Flood hazard assessment and mapping of flood inundation area of the Awash River Basin in Ethiopia using GIS and HEC-GEORAS/HEC-RAS Model. J Civ Environ Eng 5(4):1–12

Gigovi´cPamuˇcarBaji´cDrobnjak LDZS (2017) Application of GIS-interval rough AHP methodology for flood hazard mapping in urban areas. Water 9(360):1–26

Greenbaum D (1985) Review of remote sensing applications to groundwater exploration in basement and regolith. In British geological survey, overseas geology series. Nottingham, UK

Hussain M, Tayyab M, Zhang J, Shah AA, Ullah K, Mehmood U, Al-Shaibah B (2021) GIS-Based multi-criteria approach for flood vulnerability assessment and mapping in district Shangla: Khyber Pakhtunkhwa Pakistan. Sustainability 2021(13):3126. https://doi.org/10.3390/su13063126

Kefyalew A (2003) Integrated flood management: case study Ethiopia. Water Resource Consultant, Ethiopia

Kowalzig J (2008) Climate, poverty, and justice: what the Poznań UN climate conference needs to deliver for a fair and effective global deal. Oxfam 4(3):117–148

Kron W (2002) Keynote lecture: flood risk = hazard exposure vulnerability. Flood defence, 82–97

Legese B, Gumi B (2020) Flooding in Ethiopia; causes, impact, and coping mechanism a review. Int J Res Anal Rev (IJRAR)

Magesh NS, Chandrasekar N, Soundranayagam JP (2012) Delineation of groundwater potential zones in Theni district, Tamil Nadu, using remote sensing GIS and MIF techniques. Geosci Front 3(2):189–196

Mezgebedingil AG, Suryabhagavan KV (2018) Developing flood hazard forecasting and early warning system in Dire Dawa Ethiopia. Int J Adv Multidiscip Res 5:11–27

Morea H, Samanta S (2020) Multi-criteria decision approach to identify flood vulnerability zones using geospatial technology in the kemp-welch catchment, Central Province. Appl Geomat 12(4):427–440. https://doi.org/10.1007/s12518-020-00315-6
Morgan RP (1995) Soil erosion and conservation. Longman, Harlow, p 198
National Meteorological Services Agency (NMSA) (2001) Initial national communication of Ethiopia to the united nations framework convention on climate change (UNFCCC), edited by Addis Ababa, Ethiopia
OFDA (2012) Annual disaster statistical review: WHO collaborating centre for research on the epidemiology of disasters
Ogato GS, Bantider A, Abebe K, Geneletti D (2020) Geographic information system (GIS)–based multi criteria analysis of flooding hazard and risk in Ambo Town and its watershed, West shoa zone, Oromia regional State Ethiopia. J Hydrol Reg Stud. https://doi.org/10.1016/j.ejrh.2019.10
Ouma YO, Tateishi R (2014) Urban flood vulnerability and risk mapping using integrated multi-parametric AHP and GIS: methodological overview and case study assessment. Water 6:1515–1545
Rimba AB, Setiawati MD, Sambah AB, Miura F (2017) Physical flood vulnerability mapping applying geospatial techniques in Okazaki city, aichi prefecture Japan. Urban Sci 1(1):7
Rincón D, Khan UT, Armenakis C (2018) Flood risk mapping using GIS and multi-criteria analysis: a greater Toronto area case study. Geosciences 8:275. https://doi.org/10.3390/geosciences8080275
Rozalis S, Morin E, Yair Y, Price C (2010) Flash flood prediction using an uncalibrated hydrological model and radar rainfall data in a mediterranean watershed under changing hydrological conditions. J Hydrol 394:245–255
Saaty TL (1980) The analytic hierarchy process. planning, priority setting, resource allocation. McGraw Hill, New York, USA
Saaty TL, Vargas LG (1991) Prediction projection and forecasting. Kluwer Academic Publishers, Dordrecht, p 251
Samela CR, Sole A, Manferda S (2018) A GIS tool for cost-effective delineation of flood-prone areas. Comput Environ Urban Syst 70:43–52
Singh AP, Arya AK, Singh DS (2020) Morphometric analysis of Ghaghara River basin, India, using SRTM data and GIS. J Geol Soc India 95(2):169–178. https://doi.org/10.1007/s12594-0201406-3
Tas E (2017) Flood risk potential assessment in akarcay sinanpasa sub basin using GIS techniques. 3rd International conference on geography, environment and GIS
Tucci CEM (2007) Urban flood management. World Meteorological Organization, Geneva
Vojtek M, Vojteková J (2019) Flood susceptibility mapping on a national scale in Slovakia using the analytical hierarchy process. Water 11:364. https://doi.org/10.3390/w11020364
Wang Y, Li Z, Tang Z, Zeng G (2011) A GIS-based spatial multi-criteria approach for flood risk assessment in the Dongting Lake region, Hunan, Central China. Water Resour Manage 25:3465–3484. https://doi.org/10.1007/s11269-011-9866-2
Ward RC, Robinson M (1990) Principles of hydrology. McGraw-Hill, London, p 365
Wondim YK (2016) Flood hazard and risk assessment using GIS and remote sensing in lower Awash sub-basin Ethiopia. J Environ Earth Sci 6(9):69–86